

***Ab initio* multiconfiguration self-consistent-field calculations of the excited states of a Mn impurity in CaF₂**

A. C. Lewandowski and T. M. Wilson

*Computational Solid State Research Laboratory, Physics Department,
Oklahoma State University, Stillwater, Oklahoma 74078*

(Received 14 December 1993)

We analyze Mn absorption in CaF₂:Mn by the employment of *ab initio* quantum-mechanical cluster calculations and ligand-field methods. The [MnF₆]⁶⁻ O_h cluster is chosen to represent the isolated Mn²⁺ substitutional impurity in an otherwise perfect crystal. The methods of unrestricted open-shell Hartree-Fock self-consistent field (SCF), Møller-Plesset perturbation theory to second- and fourth-order, and singles and doubles configuration interaction are used to calculate the spin sextet and quartet ground states. With the active space consisting of the Mn 3*d* molecular orbitals, the spin quartet excited states are calculated by the method of multiconfiguration SCF. It was found that the presence of an external field designed to reproduce the Madelung potential difference within the cluster did not significantly affect the Mn *d*-to-*d* transitions. The crystal-field term splitting diagrams for the eight-coordinated Mn²⁺ impurity in O_h symmetry are calculated. The results showed a narrowing of the multiplet terms in energy with respect to the six-coordinated O_h result. This increases the crystal-field parameter *Dq* from the previously published value of 420–570 cm⁻¹.

I. INTRODUCTION

With its introduction as a highly efficient thermoluminescent radiation dosimeter by Ginther and Kirk in 1957,¹ CaF₂:Mn has been the subject of much study because of the wide-range linearity of its thermoluminescent response to radiation dose and the location of a major glow peak well above room temperature. While much of the early work centered around the operational importance of CaF₂:Mn and its use in dosimetry,^{2–5} it was not until the last two decades that detailed studies became available as to the role 3*d* ions play in altering the optical properties of CaF₂. The purpose of these studies has been to examine the processes of energy storage in this material following irradiation and the subsequent release of this energy in the form of luminescence. With regard to Mn in particular, optical absorption,^{6–9} photoluminescence,^{6,10–12} and thermoluminescence^{1,8,13–15} (TL) studies have led to a wealth of experimental data from which different models and energy level assignments have been put forward. For instance, CaF₂:Mn irradiated at room temperature is characterized by one main TL glow peak near 550 K. If irradiated at 80 K, a second more intense peak at 200 K appears.¹⁵ The emission spectra of both peaks indicate a process which involves the relaxation of an excited *Mn²⁺ ion to a ground state Mn²⁺ ion producing an emission peak at 495 nm. A peak at this same wavelength from photoluminescence measurements has been assigned to a transition from the ⁴T_{1g}(⁴G) level of the Mn²⁺ ion.¹⁰ X-ray-induced luminescence has also been shown to emit at the same wavelength.^{6,11}

Of particular interest is the work of McKeever *et al.*⁹ They describe a series of Mn absorption studies in CaF₂

with varying levels of Mn dopant before and after irradiation. Before irradiation they observe optical absorption spectra characteristic of internal Mn²⁺ transitions. After irradiation they observe not only an increase in the intensity of the absorption by 10³ but also the creation of new structure which is explained in terms of substitutional Mn²⁺ becoming associated with radiation-induced defects such as *F* centers.⁹ They propose a model for which the adjacent *F* center breaks the O_h symmetry of the isolated substitutional Mn²⁺ impurity and the additional *F*-center electron couples with the 3*d*⁵ electrons in Mn²⁺ thereby removing the spin and parity forbiddance of optical transitions resulting in a greatly enhanced and more complex absorption pattern.⁹

While the available experimental data has gone far in illuminating the processes involved and has led to the proposal of a plausible qualitative model of the defects involved, the present state of research has reached a point where quantum-mechanical calculations could contribute greater insight. The employment of quantum-chemical computational techniques now represent the next logical step in the understanding of these processes.

Molecular orbital calculations of defect clusters within the Hartree-Fock formalism and its extensions such as configuration interaction (CI), Møller-Plesset many-body perturbation theory to second (MP2) and fourth order (MP4), and multiconfigurational self-consistent-field (MCSCF) techniques have been incorporated into the GAUSSIAN 92 (Ref. 16) general purpose quantum-chemical program. With the recent incorporation of external charge distributions and an effective treatment of *d* electrons, large scale calculations of the electronic structure of both the ground and excited states of defect clusters in crystals containing 3*d* ions can now be accomplished. This is also facilitated by the recent widespread availabil-

ity of relatively inexpensive high-speed electronic computers.

The purpose of this paper is to analyze the Mn absorption spectrum in CaF₂ using the results of calculations of both the ground and excited states of an isolated Mn²⁺ impurity (that is, before the sample would be irradiated). The methods employed to determine the spin sextet and quartet ground states include unrestricted Hartree-Fock (UHF), restricted open-shell Hartree-Fock (ROHF), CI, MP2, and MP4. The method of MCSCF is used for the calculation of the spin quartet excited state energy levels. The resulting multiplet levels are then compared to the experimental optical absorption spectra. To our knowledge, this is the first *ab initio* calculation of the Mn absorption spectra in CaF₂.

In addition to the above calculations, the ligand-field Tanabe-Sugano¹⁷ diagrams of the eightfold-coordinated Mn²⁺ impurity with *O_h* symmetry will be developed. It is to be noted that while ligand-field theory has been applied to this system before,^{9,10} the Tanabe-Sugano diagrams used in the analysis were for six-coordinated *O_h* 3*d* ions. From group theory it is evident that the same terms will arise from both the six- and eight-coordinated systems; however, the spacing of the terms in energy will be affected by the coordination number and we show that this leads to a larger *Dq* crystal-field splitting parameter than has thus far been reported in the literature.^{9,10}

II. METHODS EMPLOYED

A. Theoretical background

The literature on the method of Hartree-Fock is extensive with numerous articles published on various aspects of the theory including several review articles and books on the subject.¹⁸⁻²² While a detailed discussion of the underlying theory of the Hartree-Fock method and its extensions is outside the scope of this paper, it will be worthwhile to briefly describe some of the essential features.

We seek to determine the solutions of the electronic Schrödinger equation within the Born-Oppenheimer approximation. The electronic Hamiltonian in atomic units describing the motion of *N* electrons in the field of *M* point charges is²¹

$$\mathcal{H} = - \sum_{i=1}^N \frac{1}{2} \nabla_i^2 - \sum_{i=1}^N \sum_{A=1}^M \frac{Z_A}{r_{iA}} + \sum_{i=1}^N \sum_{j>i}^N \frac{1}{r_{ij}}. \quad (1)$$

Within a molecular orbital picture, the Hartree-Fock approximation assumes an antisymmetric wave function in the form of a single Slater determinant which is the simplest form of the wave function that satisfies the antisymmetry requirement. This Slater determinant introduces so-called exchange effects whereby the motion of two electrons with parallel spins are correlated; however, the motion of electrons with opposite spins remain uncorrelated.²¹ It is the purpose then of the various extensions to Hartree-Fock theory such as CI, MP2, MP4,

and MCSCF to build in the missing correlation energy.²⁰

Hartree-Fock theory results in a set of one-electron nonlinear Hartree-Fock eigenvalue equations which must be solved iteratively utilizing the self-consistent-field (SCF) method. The SCF procedure begins by making an initial guess of the spin orbitals. One method is to determine the starting orbitals by diagonalizing a noninteracting Hamiltonian of the form $\mathcal{H} = \sum_{i=1}^N h(i)$ where the operator $h(i)$ describes the kinetic and potential energy of electron *i*. Once the initial spin orbitals are determined the Hartree-Fock potential $v^{\text{HF}}(i)$ is calculated and the Hartree-Fock eigenvalue equations are solved for the new set of spin orbitals from which one calculates the new average potential and then the Hartree-Fock eigenvalue equations are solved again. This procedure is continued until the spin orbitals used to construct the Fock operator are the same as its eigenfunctions. At this point self-consistency is achieved.

This procedure produces a set of orthonormal spin orbitals χ_k and a set of one-electron orbital energies ϵ_k . The Slater determinant formed from the *N* spin orbitals with the lowest orbital energies will be the Hartree-Fock ground state and is the best variational approximation to the ground state of the system of a single determinant form. The remaining unoccupied spin orbitals (known as virtual orbitals) correspond to the one-electron solutions to the *N* + 1 problem and are used in the CI and MCSCF procedures to improve upon the Hartree-Fock ground state solutions and to calculate excited states of the system.

While in the abstract, the Hartree-Fock equations have an infinite number of solutions; for practical molecular calculations the Hartree-Fock equation is solved by the introduction of a finite set of spatial basis functions. The spatial parts of the molecular spin orbitals (i.e., the solutions to the Hartree-Fock equations for molecular systems) are expanded in terms of the chosen basis set. Over the last two decades molecular calculations based on the Gaussian basis set have enjoyed the most success stemming mainly from the ease with which the multicenter integrals may be evaluated.^{20,21} While Gaussian functions do not have the proper behavior near the center of the nucleus about which they are located as do the Slater-type orbital basis set, it has been demonstrated that a single Slater-type orbital may be represented to an adequate approximation by a linear combination (contraction) of three or more Gaussians. Even though this represents an increase in the overall size of the basis set, the ease with which the multicenter integrals may be evaluated more than compensates. A common practice is to choose the Gaussian basis set from the published results of atomic calculations²³ and then augment this basis by more diffuse *s*, *p*, and *d* Gaussian-type functions.

The introduction of the finite basis converts the above abstract operator equation into a matrix eigenvalue problem. When the spatial parts of the spin molecular orbitals are constrained to be the same for both the up (α) and down (β) spins the method is known as restricted Hartree-Fock (RHF) and the resulting matrix equations are called Roothaan equations.^{20,21} By allowing the spatial parts for α and β spins to differ the method is known

as unrestricted Hartree-Fock (UHF) described by the Pople-Nesbet matrix equations.^{20,21} Both methods were used in calculations presented in this paper and both have been implemented in the GAUSSIAN 92 (Ref. 16) system of quantum-chemistry programs.

As already mentioned, in Hartree-Fock theory the motion of electrons with opposite spins are not correlated. This is a consequence of the single determinantal form of the variational wave function and as a result even for an infinite basis set the ground state Hartree-Fock energy will always lie above the exact nonrelativistic Born-Oppenheimer ground state energy by the amount of energy involved in this missing correlation. One important method used to obtain this missing correlation energy is the method of configuration interaction (CI). While CI is a well-known method and has been described in detail elsewhere,^{20,21} it will be useful to summarize the essential features.

For a basis set consisting of K basis functions the Hartree-Fock procedure will produce $2K$ molecular spin orbitals. For N electrons, the ground state Hartree-Fock wave function will be a single Slater determinant comprised of the N lowest-energy spin orbitals. Representing this ground state wave function as,²¹

$$|\Psi_0\rangle = |\chi_1, \chi_2 \cdots \chi_a \chi_b \cdots \chi_N\rangle, \quad (2)$$

where it is understood that the remaining $2K - N$ spin orbitals are unoccupied, it is clear that the determinant given by Eq. (2) is but one of many N -electron determinants that could be formed from the $2K$ spin orbitals. For instance, one could form a singly excited determinant by promoting an electron from the occupied spin orbital χ_a into the previously unoccupied virtual spin orbital χ_r producing the wave function

$$|\Psi_a^r\rangle = |\chi_1, \chi_2 \cdots \chi_r \chi_b \cdots \chi_N\rangle, \quad (3)$$

where the notation $|\Psi_a^r\rangle$ designates that the spin orbital χ_a in the ground state Hartree-Fock wave function has been replaced by the virtual spin orbital χ_r . A doubly excited determinant could be produced by exciting electrons from χ_a and χ_b to χ_r and χ_s thus

$$|\Psi_{ab}^{rs}\rangle = |\chi_1 \chi_2 \cdots \chi_r \chi_s \cdots \chi_N\rangle. \quad (4)$$

In fact the total number of determinants that could be produced in this way is $(2K)!/[N!(2K - N)!]$. While the excited determinants do not in themselves represent the excited states of the system, they do form N -electron basis functions in which the exact N -electron states may be expanded. If $|\Phi\rangle$ is the exact wave function of the system for a given basis, then the CI expansion would be²¹

$$|\Phi\rangle = c_0|\Psi_0\rangle + \sum_{ra} c_a^r |\Psi_a^r\rangle + \sum_{\substack{a < b \\ r < s}} c_{ab}^{rs} |\Psi_{ab}^{rs}\rangle + \sum_{\substack{a < b < c \\ r < s < t}} c_{abc}^{rst} |\Psi_{abc}^{rst}\rangle + \cdots \quad (5)$$

Diagonalizing the CI matrix $\langle \Psi_i | \mathcal{H} | \Psi_j \rangle$, where $\{|\Psi_i\rangle\} = \{|\Psi_0\rangle, |\Psi_a^r\rangle, |\Psi_{ab}^{rs}\rangle, \dots\}$, gives not only the lowest possible upper bound to the ground state energy but also

the lowest possible upper bounds to the excited states of the same spin for the given basis set.²⁴ While the CI approach is systematic, the number of determinants required to represent all excitations becomes extremely large for even small systems. For most practical calculations the CI expansion Eq. (5) is commonly truncated to include only up to at most triple excitations.

For the CI calculations presented in this paper, CI singles (CIS), consisting of only the single excitations in Eq. (5), will be used as an aid for determining the Hartree-Fock ground state. In addition, the method of CI using both single and double substitutions of the determinant (CISD) will be used to calculate the ground to first excited state transition energy.

A variation on this theme is the method of multiconfigurational SCF (MCSCF). This method is a combination of CI and SCF. It is in fact SCF with a multideterminantal wave function obtained from a full CI expansion within a selected manifold of molecular spin orbitals known as the active space.²⁰ When the truncated CI expansion is constructed out of all possible configurations within the specified active space, the method is known as complete active space SCF (CASSCF). With this understood, we will use the term MCSCF synonymously with CASSCF. Thus the MCSCF is a truncated CI expansion in which both the expansion coefficients and the molecular orbitals for all the electrons are optimized.^{25,26} The added advantage is that the orbitals may be optimized for each excited root and thereby, with the proper choice of the active space, one may obtain excited state energies of the same spin multiplicity. For this reason MCSCF is a powerful computational tool for the calculation of a system's multiplet structure.

B. Cluster geometry and basis set

Mn^{2+} ions enter the CaF_2 lattice substitutionally and are surrounded by eight F^- ions arranged in O_h symmetry. To model the isolated Mn impurity, we construct a cluster consisting of a central Mn^{2+} ion and the nearest neighbor F^- ions as shown in Fig. 1. With the Mn^{2+} ion at the origin the F^- ions are located at $(\pm \frac{a}{2}, \pm \frac{a}{2}, \pm \frac{a}{2})$, where a is the F-F distance. Recent experimental evidence in the form of x-ray absorption near-edge structure (XANES) (Ref. 27) indicates a first shell Mn-F distance of 2.20 Å. This represents about a 7% inward relaxation

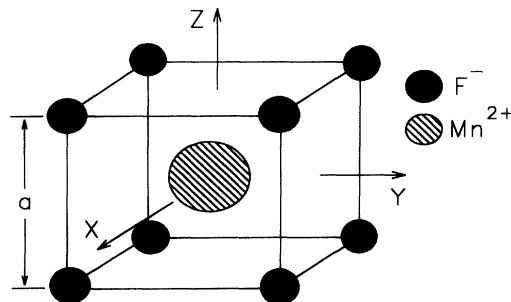


FIG. 1. Diagram of the $[\text{MnF}_8]^{6-}$ cluster used to model the isolated Mn impurity in CaF_2 .

of the nearest neighbor fluorine ions from the perfect CaF_2 Ca-F nearest neighbor distance of 2.366 \AA .²⁸

The choice of the variational basis set is perhaps the most important consideration when attempting to perform accurate SCF calculations for many-electron systems. Basis set related errors have been reviewed extensively in the literature.²⁹ One attempts to choose a basis that, while limited enough in size for practical calculations, is also flexible enough so as not to unduly bias the results. Particular attention must be paid to the Mn $3d$ orbitals as they are the ones primarily responsible for the observed transitions. The Hartree-Fock SCF procedure attempts to find the lowest energy of a given spin and spatial symmetry. However, the SCF procedure may not initially converge to the ground state of a given basis but may get trapped in a local minimum. This is related to the fact that if the charge density of the initial guess is substantially removed from the ground state charge density the finite basis set may not allow for a smooth transition from the initial guess to the ground state. As a result it is sometimes necessary to alter the occupied orbitals in a series of SCF calculations. As will be discussed in the following section, a CI singles (CIS) procedure provides a systematic method for doing this.

The standard basis functions used for atomic calculations of the F^- ion and the Ca and Mn atoms from Huzinaga *et al.*²³ provide a starting point for choosing a basis. The core orbitals were constructed from this source and then were augmented by the addition of more diffuse s , p , and d Gaussian-type functions. In total, 9 atomic basis functions were used for fluorine, 13 for calcium, and 23 for manganese. The atomic basis functions each consist of a linear combination (contraction) of Gaussian-type functions which are a product of a radial Gaussian and a real spherical harmonic function.

C. External field

It has been pointed out that in many cases the modeling of crystal defects by isolated cluster calculations can lead to inaccurate results.³⁰ While this may certainly be true for defect complexes where the electron charge density is delocalized in, for instance, an F center, or for materials exhibiting a large degree of covalent bonding, one expects this problem to be less severe for point impurities in ionic crystals. This is borne out by the success to which the method of ligand fields has had in its application to transition metals in the alkali halides and alkali earth fluorides. Nevertheless, in every case it must be demonstrated to what degree the external field affects the calculated transitions.

To a first approximation, an external arrangement of point ions must produce the Madelung potentials within the cluster. For a finite external arrangement, however, this requires a judicious choice of the external point ion distribution cutoff radius. The Madelung potentials for CaF_2 available in the literature²⁸ are $\phi_{\text{F}}^{\infty} = 0.394$ hartree for a F site and $\phi_{\text{Ca}}^{\infty} = -0.733$ hartree for a Ca site. The ∞ superscript is used to indicate the potentials for an infinite lattice. A finite external arrangement of point

ions must be chosen such that it produces the cluster-subtracted Madelung potentials at the Mn and F sites within the quantum cluster. Accounting for the electrostatic contributions to the Madelung potential due to the cluster ions the cluster-subtracted Madelung potentials are $\phi_{\text{F}}^{\infty'} = 1.051$ hartree and $\phi_{\text{Mn}}^{\infty'} = 1.056$ hartree. The external lattice size therefore will be chosen such that its potential reproduces the difference $\phi_{\text{Mn}}^{\infty'} - \phi_{\text{F}}^{\infty'} = 0.005$ hartree.

For these calculations, the external field was produced by arranging outside the quantum cluster -1 and $+2$ point charges representing the F^- and Ca^{2+} ions, respectively. These external ions were situated so as to conform to the structure of a perfect CaF_2 lattice. Figure 2 shows the potential difference $\phi'_{\text{Mn}}(R) - \phi'_{\text{F}}(R)$ as a function of the radius of the external arrangement of point ions from the central Mn ion. This figure shows that as the size of the external arrangement increases, the potential difference begins to converge as one would expect. As the size is further increased, one would expect the potential difference produced from the finite arrangement to approach the value for the infinite lattice, namely 0.005 hartree. The goal of modeling the infinite lattice with a finite arrangement of point ions can be achieved by selecting the size of this finite arrangement so that the potential difference produced by it most closely matches the value for the infinite lattice. Figure 2 shows that this is accomplished with an external point ion radius of 20.647 bohrs consisting of 412 point ions. This arrangement produced the desired potential difference of 0.005 hartree.

D. Methodology

The cluster under consideration in Fig. 1 has an overall charge of -6 . Each F^- has closed $2p$ shells and the

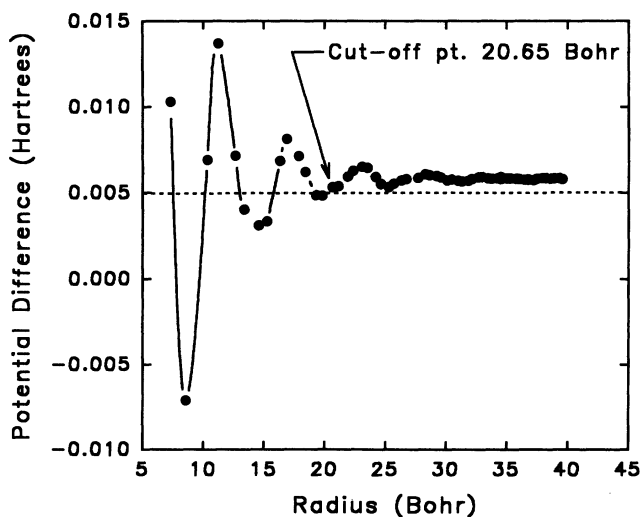


FIG. 2. The electrostatic potential difference between the central Mn site and a F site, $\phi'_{\text{Mn}}(R) - \phi'_{\text{F}}(R)$, as a function of the radius of the external point ion arrangement from the central Mn ion. As shown in the figure, the arrangement actually used for the SCF calculations consisted of those external point ions less than 20.65 bohrs from the central Mn site.

Mn^{2+} has the $3d^5$ configuration outside closed shells. The ground state is the ${}^6A_{1g}(t_{2g}^3e_g^2)$ term with the term ${}^4T_{1g}(t_{2g}^2e_g^3)$ as the first excited state which is the spin quartet ground state. The methodology used for SCF calculations presented in this paper involves essentially four steps: (i) For the given external field, perform a series of SCF and CIS calculations to obtain the ground state for a given spin multiplicity, (ii) optimize the basis set to minimize the ground state energy, (iii) use electron correlation methods such as MP2, MP4, and CISD to improve upon the ground state energies, and, (iv) use the method of MCSCF to calculate the excited state energies within the spin 3/2 manifold of states. Along the way, an important question one must answer is the degree by which the external field affects the electronic transition energies. Also, so as to reduce the computational task, we performed the CISD calculations under the frozen core restriction. Under this restriction, the excitations in the CISD expansion are not taken from the core molecular orbitals. For the calculations presented in this paper the molecular orbitals designated as core consisted of the Mn^{2+} $1s$ -, $2s$ -, and $2p$ -type molecular orbitals and the eight F^- $1s$ -type molecular orbitals.

To obtain the ground state ${}^6A_{1g}({}^6S)$, we started from an initial guess generated by diagonalizing the core Hamiltonian. As already stated above, this method of generating an initial guess generally produces a charge density that is significantly removed from the converged Hartree-Fock density for the ground state. Furthermore, since the basis set is finite, the SCF procedure generally will not converge to the ground state on the first attempt. One method of overcoming this problem is to perform a Hartree-Fock SCF calculation and then do singles CI. This will produce the CIS energy spectrum and the leading coefficients for the singles CI expansion. From the energy spectrum one may determine the approximate energy of those states with the same spin multiplicity below the SCF-converged result and, from the leading coefficients in the CI expansion, determine which molecular orbital alterations need to be made to the guess for the next SCF-CIS calculation. This procedure is continued until CIS does not produce an energy below the present SCF-converged result. Of course, the ground states for some spin multiplicities are multideterminantal [such as ${}^4T_{1g}({}^4G)$]; in this case CIS will always give a lower energy. For this case CIS will produce a lower-energy eigenvalue; however, the CI expansion will contain several determinants with similar expansion coefficients indicating that the wave function is best described as a linear combination of determinants. At this point, it is unlikely that further alterations will lead to a lowering of the SCF energy and hence the Hartree-Fock ground state single determinantal wave function is obtained.

With the ground state determined, the next step is to optimize the basis set. For these calculations, this is done by repeatedly performing SCF calculations with the Gaussian exponents varied each time so as to lower the SCF energy. The GAUSSIAN 92 (Ref. 16) quantum-chemical programs provide a utility for just this type of operation. In practice only the basis functions representing the valence electrons are varied. Once the basis set

is optimized for the ground state, the first excited state ${}^4T_{1g}({}^4G)$ is obtained by flipping a spin and following the SCF-CIS procedure outlined above.

The Hartree-Fock wave functions are then improved upon by utilizing the correlated methods of MP2, MP4, and CI including single and double substitutions. The results are given in the following section. In addition, calculations were performed to test the effect of the external field on the ground state to first excited state transition energy.

Finally the method of MCSCF is used to calculate the excited state energies within the spin 3/2 manifold of states. The choice of the proper active space for MCSCF is of utmost importance. For these calculations, the active space was chosen so that all orbitals correspond to the N -electron problem in the following fashion. Currently MCSCF, as implemented by GAUSSIAN 92,¹⁶ is a spin-restricted procedure. Therefore a restricted open-shell Hartree-Fock (ROHF) calculation of the ${}^6A_{1g}({}^6S)$ ground state is first performed. This state is spin 5/2 with all five $3d$ electrons spin aligned. Choosing the active space to be these five spin-restricted $3d$ molecular orbitals (MO's) and flipping one spin so as to produce the spin 3/2 first excited state, the active space now consists of five electrons and five MO's except that now one MO is doubly occupied and one MO is empty. Since the empty MO was obtained from the spin 5/2 calculation, it still corresponds to the N -electron problem and is therefore, strictly speaking, not a virtual MO. The complete active space expansion produces 24 distinguishable determinants with which to represent the spin 3/2 states. The results of the MCSCF calculations are presented in the next section.

Finally, as already discussed, ligand-field theory has been applied to this system before.⁹ However, the Tanabe-Sugano diagrams used for the analysis were for O_h six-coordinated Mn. Therefore, one aspect of this work was to determine the proper diagrams for eight-coordinated Mn and discuss both the MCSCF results and experimental data in terms of the new diagrams. These results are presented in the next section and a summary of the theory is presented in Sec. IV B.

III. RESULTS

In Table I we present a summary of the ground state to first excited state transition energies obtained experi-

TABLE I. Values of the transition energy from the ground state [${}^6A_{1g}({}^6S)$] to the first excited state [${}^4T_{1g}({}^4G)$] obtained from the various methods employed. The experimental results are from McKeever *et al.* (Ref. 9).

Method	${}^6A_{1g}({}^6S) \rightarrow {}^4T_{1g}({}^4G)$ (eV)
Experimental	2.81
UHF (with ext. field)	3.71
UHF	3.76
MP2	3.53
MP4	3.49
CISD	3.46
MCSCF	3.54

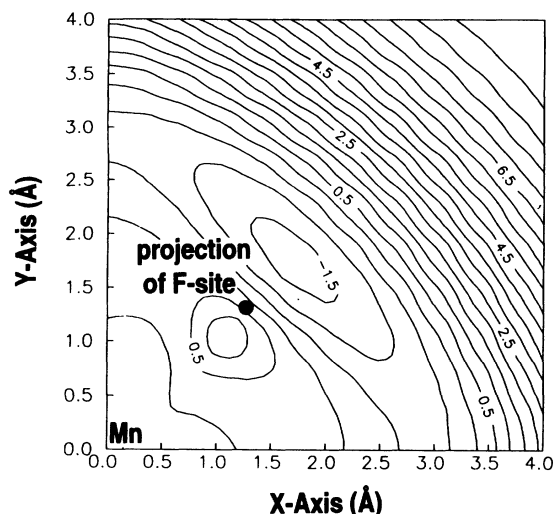


FIG. 3. The percent change in the electronic charge density in the x - y plane defined in Fig. 1. This figure shows that within the confines of the quantum cluster the percent change in the electronic charge density arising from the introduction of the external point ion field is no more than $\sim 1\%$.

mentally and from the various quantum-chemical methods. One point to note is that at the UHF level of theory, the calculated transition energies both with and without the external field differ by only 0.05 eV. As we will point out later, this difference is slightly higher than the resolution obtainable in these calculations from the MCSCF technique for the excited states. We may conclude, therefore, that as far as the transition energies are concerned, the effect of the external field is quite small. This observation is consistent with studies of Mn centers in other hosts such as ZnS by Richardson and Janssen,³¹ by Flórez *et al.*³² in RbMnF₃, and V²⁺ in ZnSe by Wilson.³³ As further evidence, Fig. 3 shows the percent change in the

electron density about the quantum cluster arising due to the effect of the external field. The percent change is calculated by $\{[\rho_{\text{ext}}(\mathbf{r}) - \rho(\mathbf{r})]/\rho_{\text{ext}}(\mathbf{r})\} \times 100$, where $\rho_{\text{ext}}(\mathbf{r})$ is the electronic charge density in the presence of the external field. The figure shows the percent change in the x - y plane as defined in Fig. 1. The location of the F⁻ ion is actually the location of its projection onto the x - y plane. The figure shows that within the confines of the quantum cluster, the percent change in the electron charge density arising from the introduction of the external point ion field is no more than $\sim 1\%$. Since the excited states are due to d -to- d transitions and since the d orbitals are rather localized about the Mn ion, one expects the presence of the external field to have little effect. Therefore, having introduced an external field and finding its effects to be negligible for transition energies, we may now proceed without the external field for further calculations.

The remaining results in Table I were calculated without an external field. While the CISD method yields the best transition energy, it is still 0.65 eV above the experimental value. An error of this magnitude for d -to- d transitions in Mn-related defects is quite common. Richardson and Janssen,³¹ for instance, report a UHF error of 1.6 eV for the ground to first excited state transition for Mn defects in ZnS. For the Mn in CaF₂, we see that the UHF error is 0.95 eV without the external field. Thus, the CISD method has accounted for approximately 0.30 eV of the missing correlation energy with the present basis. Part of the missing correlation effects can be accounted for at the MP4 and CISD levels of theory by increasing the size of the basis set. With the present basis, however, one could obtain somewhat improved results through either a single reference MCSCF+CI (see, for instance, Luth and Scheiner³⁴) or the multireference CI method which involves performing CI (usually up to CISD) from selected configurations determined from a previous MCSCF calculation.³⁵ However, the application

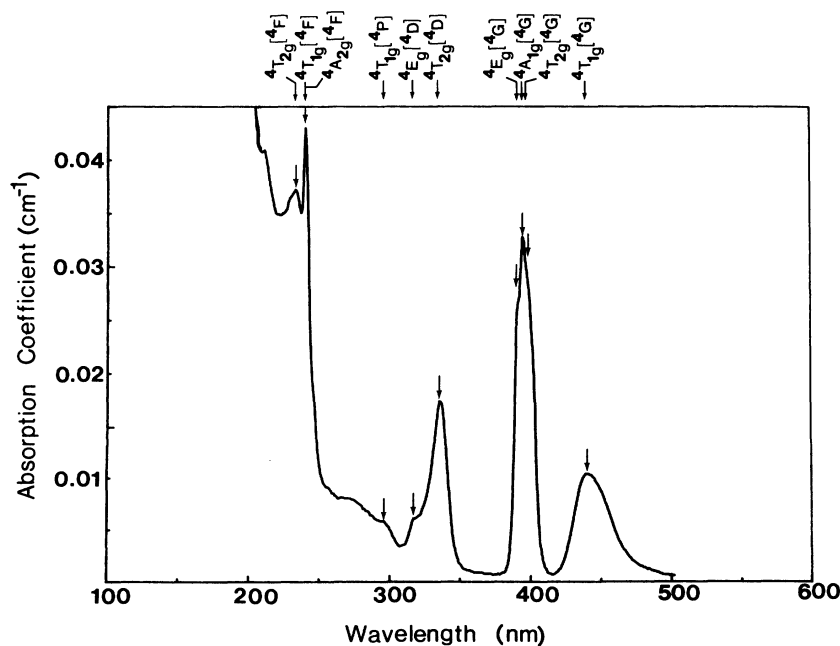


FIG. 4. Optical absorption of an unirradiated specimen of CaF₂:Mn (3%). The absorption peaks have been assigned to the multiplet terms arising from the free ion energy levels 4G , 4D , 4P , and 4F as described in the text [McKeever *et al.* (Ref. 9)].

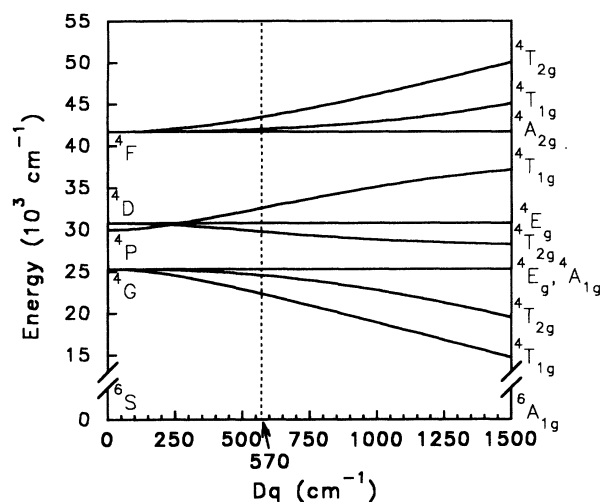


FIG. 5. Crystal-field splitting diagram for the d^5 system in $O_h^{(8)}$ symmetry for $B = 781 \text{ cm}^{-1}$ and $C = 3.498 \times 10^3 \text{ cm}^{-1}$. The energies are presented with respect to the ground state ${}^6A_{1g}({}^6S)$. The dashed line shows the value of Dq that gives the best fit to the experimental data of McKeever *et al.* (Ref. 9).

of the multireference methods for systems of this size remains a formidable computational task and therefore were not included in this study. A final observation from Table I is that the MCSCF technique is at the same level as MP2 as far as correlation is concerned.

In Fig. 4 we show the optical absorption data by McKeever *et al.*⁹ Their experimental values are presented in Table II as column 4. The assigned term designations were made by them based on a ligand-field analysis from fitting to the $3d^5$ Tanabe-Sugano diagram for an ion in the presence of a point ion field of O_h (six-coordinated) symmetry. This resulted in a Dq value of 420 cm^{-1} for the crystal-field splitting parameter.⁹ We have reworked the Tanabe-Sugano diagram for a $3d^5$ eight-coordinated O_h system in Sec. IV B. We present the results as Fig. 5. The dashed line shows the Dq value that gives the best fit to the new diagram using the experimental data of column 4 of Table II. This results in a new Dq value of 570 cm^{-1} .

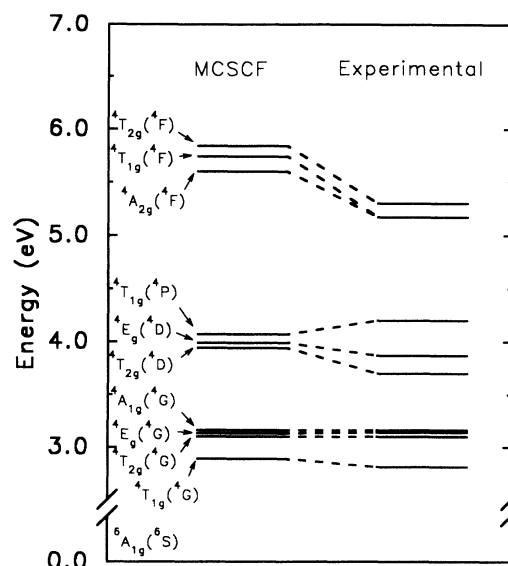


FIG. 6. Graphical representation of the numerical MCSCF results presented in Table II after the -0.647 eV rigid shift. The experimental results are from McKeever *et al.* (Ref. 9).

Table II shows the results of MCSCF calculations. The second column gives the transition energies from the ground state calculated at the ROHF level of theory to the excited states calculated at the MCSCF level of theory. We note that as one moves up in energy with successive MCSCF calculations, one observes the clustering of the excited state levels into the two- and threefold degeneracies of the various 4E_g , ${}^4T_{1g}$, and ${}^4T_{2g}$ terms. Because of the finite basis set and the fact that the O_h symmetry of the Mn impurity had to be relaxed in the MCSCF calculations, the energies of the partners to the irreducible representations of the O_h group indicated in column 1 will no longer be exactly degenerate. The errors shown in Table II indicate this spread in energy. The energy given in column 2 is taken as the average energy of these partners. Based upon the results of ligand-field theory and the groupings of the levels calculated by the MCSCF technique, we were able to make the term assignments in column 1 of Table II.

TABLE II. Summary of the transition energies obtained from MCSCF. The energies are with respect to the ground state ${}^6A_{1g}({}^6S)$ ROHF energy. The experimental results are from the work of McKeever *et al.* (Ref. 9).

State	Energy (eV)	After rigid shift of -0.647 eV	Experimental (eV)
${}^4T_{1g}({}^4G)$	3.54 ± 0.02	2.89 ± 0.02	2.81
${}^4T_{2g}({}^4G)$	3.75 ± 0.01	3.10 ± 0.01	3.10
${}^4E_g({}^4G)$ [${}^4A_{1g}$] ^a	3.78 ± 0.01	3.13 ± 0.01	3.14
${}^4A_{1g}({}^4G)$ [4E_g] ^a	3.81	3.16	3.16
${}^4T_{2g}({}^4D)$	4.59 ± 0.01	3.94 ± 0.01	3.70
${}^4E_g({}^4D)$	4.64 ± 0.03	3.99 ± 0.03	3.87
${}^4T_{1g}({}^4P)$	4.72 ± 0.03	4.07 ± 0.03	4.20
${}^4A_{2g}({}^4F)$	6.25	5.60	5.17
${}^4T_{1g}({}^4F)$	6.39 ± 0.03	5.74 ± 0.03	5.17
${}^4T_{2g}({}^4F)$	6.49 ± 0.02	5.84 ± 0.02	5.30

^aAssignments made by McKeever *et al.* (Ref. 9).

From Fig. 4 we observe that experimentally some energies are known better than others. Since the peak designated ${}^4A_{1g}({}^4G)$ is the sharpest and hence provides the most precise experimental energy, the calculated values are rigidly shifted by -0.647 eV to match the experimental ${}^4A_{1g}({}^4G)$ level. These results are given in column 3. Figure 6 shows graphically the calculated values of column 3 and experimental values of column 4.

IV. DISCUSSION

A. MCSCF results

The *ab initio* determination of the electronic structure of the ground and excited states of complicated many-electron systems such as the $[\text{MnF}_8]^{6-}$ cluster require the employment of quantum-mechanical methods that go beyond the Hartree-Fock level of theory. Since large scale CI calculations are impractical for systems of this size, the only practical alternative is the complete active space multiconfigurational SCF method. It is then the intent of this work to demonstrate that the MCSCF technique produces reliable transition energies that are in good agreement with experiment. The active space chosen to calculate the excited states for the $[\text{MnF}_8]^{6-}$ cluster within the spin 3/2 manifold of states consists of the Mn *d*-like molecular orbitals. In all, this produced 24 configurations. The MCSCF technique then starts with the ROHF orbitals, diagonalizes the CI matrix consisting of the 24 configurations, and produces the CI expansion coefficients and eigenvalues. Then, with the wave function represented by this truncated CI expansion, the orbitals are then varied so as to minimize the desired eigenvalue. With the new orbitals, the CI matrix is diagonalized again and the process is repeated until the desired eigenvalue converges. Since at every step of the way the CI eigenvalues are rigorous upper bounds to the excited state energy, by choosing to optimize the orbitals for one of the excited CI eigenvalues, one obtains the best possible excited state energy for the given active space.

Table II shows the results of the MCSCF calculations for all of the Mn $S=3/2$ states. Figure 6 shows the same results graphically. With regard to these results there are two important points. First, it was found that the MCSCF method does a much better job predicting the *relative* spacing of the energy levels within a given spin manifold than it does in predicting the absolute transition energies. Column 2 in Table II gives the energies of the spin 3/2 states with respect to the spin 5/2 ground state. By comparing these values with the experimental results in this table, we see that they depart from the experimental values by on the average of about 1 eV. By performing a rigid shift of -0.647 eV to match the experimental ${}^4A_{1g}({}^4G)$ level the overall agreement as shown in Fig. 6 is much better. We note that within the 24-configuration MCSCF approach adopted in this work for the spin 3/2 states, only the *d-d* correlation energy contributions have been explicitly included. It should further be noted that for this choice of using only the *d*-like MO's to form the configurations, the ${}^6A_{1g}({}^6S)$

level can only be treated at the ROHF level of theory. Since this level is spin 5/2 with all five spins aligned, constructing the active space from the Mn *d*-like molecular orbitals produces only one possible configuration. This means that if the spin 3/2 and spin 5/2 levels are to be treated at the same level of theory (as they must for purposes of comparison) the ${}^6A_{1g}({}^6S)$ is represented by a single determinantal wave function while the quartet levels are represented by a multideterminantal wave function consisting of 24 determinants. This is roughly equivalent to doing an SCF ligand-field CI calculation in Richardson and Janssen's terminology.³¹ In their study of ZnS:Mn, they show there to be additional correlation energy corrections (CEC's) to the ($S=5/2 \rightarrow S=3/2$) transition energies of ~ 1 eV. They found the CEC's for the ${}^6A_1 \rightarrow {}^4T_1$ transition to be 0.79 eV. These corrections arise from atomic differential correlation effects for the $3d^5$ states of the free Mn^{2+} ion. From Table I we show the ${}^6A_{1g}({}^6S) \rightarrow {}^4T_{1g}({}^4G)$ transition energies for the different levels of theory. We observe that the best calculated value is obtained from a large configuration interaction calculation involving all noncore single and double substitutions (CISD). Our MCSCF results for the ${}^6A_{1g} \rightarrow {}^4T_{1g}$ transition energy is 0.73 eV greater than is observed experimentally. The CISD result reduces this error by 0.08–0.65 eV. Further, significant reductions would result were it possible to perform full CI calculations on these two states. Such calculations are not yet feasible for systems of this size. Thus the introduction of the -0.647 eV rigid shift into the MCSCF results should be viewed as a correlation energy correction. An alternative approach would be to introduce the CEC's by the method employed by Richardson and Janssen.³¹

The second point is that as one moves up in energy the calculated results begin to depart further and further from the experimental values. As one tries to calculate excited states with higher and higher energies the finite size of the active space becomes more and more relevant. This is because the higher roots, while rigorous upper bounds, are also orthogonal to the lower roots as determined using the same basis as that obtained by the MCSCF procedure for the optimized root. This, therefore, introduces an additional error into the result that increases as higher roots are optimized. Also, it is to be expected that errors involving the lack of correlation due to charge transfer contributions should be more important for the higher states. The solution that could be consistently applied to all the states would be to increase the size of the active space to include some F^- *s*- and *p*-like molecular orbitals and recalculate the states. However, this increase in the size of the active space would significantly increase the number of configurations and computational time.

According to ligand-field theory, we see from Fig. 5 that the ${}^4E_g({}^4G)$ and ${}^4A_{1g}({}^4G)$ terms remain degenerate under variations in the crystal-field splitting parameter Dq . Experimentally, of course one will observe a small separation in these terms. From Fig. 4 we observe that McKeever *et al.*⁹ assigns ${}^4A_{1g}({}^4G)$ to be the lower energy of these two terms. From the grouping of the MCSCF energy levels, however, we find that ${}^4E_g({}^4G)$ is the lower

in energy of the two terms. Consequently, based on our MCSCF calculations we reverse the term assignments of these two levels relative to the published assignments.⁹

As one moves beyond ligand-field theory the ${}^4A_{1g}({}^4G)$ and ${}^4E_g({}^4G)$ terms will split. For instance, Ng and Newman³⁶ examine a spin-correlated crystal-field model designed to include covalency effects. They found that this model places the ${}^4E_g({}^4G)$ level below the ${}^4A_g({}^4G)$ level. We also note that a refined ten-parameter treatment for $3d$ transition metal ions in crystals has been developed based on the Racah irreducible tensor operator method.³⁷ This theory also results in the lifting of the accidental degeneracy of these two levels for the $Mn^{2+} 3d^5$ system.³⁸ In addition, Ferguson, Krausz, and Guggenheim,³⁹ using magnetic circular dichroism measurements, found that in $KMgF_3:Mn^{2+}$, the ${}^4E_g({}^4G)$ level lies approximately 90 cm^{-1} below the ${}^4A_g({}^4G)$ level. Thus MCSCF predicts the proper ordering of these levels.

B. Ligand-field theory

The electronic excited states of defects involving transition metal ions in crystals is commonly analyzed using the ligand-field method. The method of ligand fields is developed in a series of papers by Tanabe and Sugano⁴⁰ and Orgel.⁴¹ Later several books and review articles appeared in the literature most notably by Sugano, Tanabe, and Kamimura,¹⁷ and Schläfer and Gliemann.⁴² These researchers discussed the splitting in the free ion terms of $3d$ ions for ligand fields with various symmetries. Essentially the ligand-field approach centers around treating the d electrons of a central ion through a screened interaction with the otherwise closed shells. The d electrons then interact via perturbation theory with a point ion external field produced by the nearest neighbor ions. This interaction results in a splitting of the free ion terms into multiplets identified by the irreducible representations of the symmetry group of the cluster. This method has enjoyed considerable success when applied to ionic crystals; however, its limitation is manifest when one begins to consider more complicated systems, such as an impurity ion adjacent to an F center in CaF_2 , for instance, if a Mn^{2+} ion enters substitutionally for Ca^{2+} and is adjacent to a vacancy in which an electron is trapped. The -1 charge of the electron in the vacancy behaves in the ligand-field point ion approximation exactly as another F^- ion surrounding the Mn impurity. Therefore, ligand-field theory would treat this system in the same way as it would treat the Mn impurity surrounded by the eight nearest neighbor F^- ions in CaF_2 .

The lowest-lying electronic level in Mn^{2+} is 6S arising from the configuration $3d^5$. In the free ion this configuration also gives rise to 4G , 4P , 4D , and 4F terms which lie $25\,000$ – $50\,000\text{ cm}^{-1}$ above the ground state.⁴³ In a crystal the quartet levels are split by the influence of the surrounding ions, the most important of which are those immediately adjacent to the central Mn^{2+} ion, the ligands. If the ligands are arranged at the corners of a regular tetrahedron, octahedron, or cube, then the strength of the ligand field may be specified by a single parameter,

usually called Dq , from which it is possible to calculate the positions of the energy levels in the crystal arising from this perturbed Mn^{2+} ion.

Some of the earliest work on Mn^{2+} surrounded by F^- ions was carried out by Stout⁴³ in his analysis of manganous fluoride. Some of the first experimental results and applications of ligand-field theory to the substitutional Mn^{2+} impurity in CaF_2 , however, was performed by Alonso and Alcalá¹⁰ in their analysis of photoluminescence excitation spectra and Bagai and Warriar⁴⁴ from ultraviolet optical absorption. However, these results lead to disagreement as to the value of Dq and the assignment of energy levels. One reason for this is that the analysis of excitation spectra is limited in the sense that these measurements are only able to observe those absorptions that give rise to luminescence. It was not until 1986 when optical absorption in the visible region was measured by McKeever *et al.*⁹ that the Mn^{2+} absorption transitions in $CaF_2:Mn$ were observed directly. From the application of ligand-field theory, McKeever *et al.*⁹ suggested a value for Dq of 420 cm^{-1} . This was in agreement with Alonso and Alcalá¹⁰ but differed significantly with the value of 810 cm^{-1} suggested by Bagai and Warriar.⁴⁴ The 420 cm^{-1} value for Dq obtained by Alonso and Alcalá and McKeever *et al.* is considered too low for it is only about 60% of those values for Dq obtained for compounds such as $RbMnF_3$, $NaMnF_3$, and MnF_2 .⁴⁵ For instance, an analysis of MnF_2 spectra led Stout⁴³ to assign a value for Dq of approximately 800 cm^{-1} for this system. Barriuso and Moreno⁴⁵ were the first to point out that the application of the published Tanabe-Sugano diagrams¹⁷ to the Mn impurity in CaF_2 may not be valid while it remains valid for the $RbMnF_3$, $NaMnF_3$, and MnF_2 compounds. The reason for this is that while the symmetry of Mn^{2+} in these compounds and in CaF_2 is O_h , Mn^{2+} is eight-coordinated in $CaF_2:Mn$ instead of six-coordinated as in the other compounds. Furthermore, since the published Tanabe-Sugano diagrams were calculated assuming the six-coordinated O_h ligand field,¹⁷ their application to eight-coordinated systems may lead to a sizable error. Since both systems have O_h symmetry, the terms arising from the ligand field will remain the same. However, since group theory can only identify the symmetry and hence the number of the resulting terms, the remaining question as to the ordering of the terms and the magnitude of the splitting as a function of Dq remained unresolved.

In this section we will briefly outline some of the principles behind ligand-field theory and describe the calculation of the term splitting diagram for a $3d^5$ ion in the presence of an electrostatic field of O_h symmetry. The field will be produced by eight point ions arranged as on the corners of a cube with the $3d^5$ ion in the center. We will denote the symmetry of the six- and eight-coordinated fields as $O_h^{(6)}$ and $O_h^{(8)}$, respectively. The energy matrices for the $3d^5$ system will be presented and diagonalized to provide the $O_h^{(8)}$ term splitting diagrams.

As far as the change from $O_h^{(6)}$ to $O_h^{(8)}$ is concerned the only change in the formalism enters into the unperturbed

Hamiltonian matrix \mathbf{H}_0 . For the $O_h^{(6)}$ system the \mathbf{H}_0 matrix consists of diagonal elements that depend only on the configuration, namely, $(6m - 4n)Dq$ for $t_{2g}^n e_g^m$. As discussed by Schläfer and Gliemann,⁴² for the $O_h^{(8)}$ system the matrix elements are given by $(4n - 6m)\frac{8}{9}Dq$. This leads to an inversion of the configurations in energy and produces a smaller magnitude in the splitting for a given value of Dq . This then leads to larger Dq values for the Mn impurity in CaF_2 than has hitherto been reported in the literature. The matrices for the interelectron interaction, \mathbf{H}_1 , remain unchanged in going from $O_h^{(6)}$ to $O_h^{(8)}$ symmetry since they only reflect the Coulomb interaction between the electrons.

In this discussion we will be interested in the sextet ground state and the quartet excited states. While the d^5 system will lead to many doublet states, experimentally transitions involving them are very weak due to their highly forbidden nature. Transitions from the ground state sextet to excited state quartets are also forbidden; however, with proper experimental techniques these have been measured.⁹ For the d^5 system the free ion terms in order of increasing energy are 6S , 4G , 4P , 4D , and 4F . By the application of group theory and spin and vector coupling methods¹⁷ we find that these free ion terms break into multiplet terms that are the irreducible representations of the O_h group. However, not all the terms allowed by group theory actually manifest themselves. Table III shows the free ion terms and the surviving O_h terms. Also shown are the configurations that give rise to those terms.¹⁷ Note that the t_{2g}^5 and $t_{2g}e_g^4$ configurations are not present since these will only lead to doublet terms.

Considering just the sextet and quartet terms, the Coulomb interaction matrices in terms of the Racah parameters for the d^5 system under O_h symmetry are given in Table IV. A common factor of A along the diagonal of each matrix is subtracted out because we will only be interested in the relative energy separations. The contribution due to the unperturbed Hamiltonian matrix \mathbf{H}_0 is included by adding a factor of $(4n - 6m)\frac{8}{9}Dq$ for $t_{2g}^n e_g^m$ along the diagonals of the Coulomb matrices in Table IV. This done, the full energy matrices can be diagonalized to find the energy eigenvalues as a function of Dq , B , C .

To complete the analysis this diagram must be compared to experimental data so that the crystal-field splitting parameter Dq can be determined. Figure 4 shows the optical absorption spectrum for $\text{CaF}_2:\text{Mn}$ (3%) obtained by McKeever *et al.*⁹ The figure shows the spectra peaks and their term assignments. From the Mn spec-

TABLE III. The surviving O_h terms arising from the sextet and quartet free ion terms for the d^5 system.

Free ion terms	O_h terms
6S	${}^6A_{1g}(t_{2g}^3 e_g^2)$
4G	${}^4T_{1g}(t_{2g}^2 e_g^3)$, ${}^4T_{2g}(t_{2g}^2 e_g^3)$, ${}^4E_g(t_{2g}^3 e_g^2)$, ${}^4A_{1g}(t_{2g}^3 e_g^2)$
4P	${}^4T_{1g}(t_{2g}^3 e_g^2)$
4D	${}^4T_{2g}(t_{2g}^3 e_g^2)$, ${}^4E_g(t_{2g}^3 e_g^2)$
4F	${}^4A_{2g}(t_{2g}^3 e_g^2)$, ${}^4T_{1g}(t_{2g}^4 e_g)$, ${}^4T_{2g}(t_{2g}^4 e_g)$

TABLE IV. The Coulomb interaction matrices for the sextet and quartet terms for the d^5 system under O_h symmetry from Tanabe and Sugano (Ref. 40). The full energy matrices to be diagonalized are obtained for $O_h^{(8)}$ symmetry by adding $(4n - 6m)\frac{8}{9}Dq$ for configuration $t_{2g}^n e_g^m$ along the diagonal.

${}^4T_{2g}({}^4F, {}^4D, {}^4G)$		
$t_{2g}^4 e_g$	$t_{2g}^3 e_g^2$	$t_{2g}^2 e_g^3$
$-17B + 6C$	$-\sqrt{6}B$	$-4B - C$
	$-22B + 5C$	$-\sqrt{6}B$
		$-17B + 6C$
${}^4T_{1g}({}^4F, {}^4P, {}^4G)$		
$t_{2g}^4 e_g$	$t_{2g}^3 e_g^2$	$t_{2g}^2 e_g^3$
$-25B + 6C$	$3\sqrt{2}B$	$-C$
	$-16B + 7C$	$-3\sqrt{2}B$
		$-25B + 6C$
${}^4E_g({}^4G, {}^4D)$		
$t_{2g}^3 e_g^2 a$	$t_{2g}^3 e_g^2 b$	
$-22B + 5C$	$-2\sqrt{3}B$	
	$-21B + 5C$	
$t_{2g}^3 e_g^2$	${}^4A_{2g}({}^4F)$	$-13B + 7C$
$t_{2g}^3 e_g^2$	${}^4A_{1g}({}^4G)$	$-25B + 5C$
$t_{2g}^3 e_g^2$	${}^6A_{1g}({}^6S)$	$-35B$

tra for several hosts it has been found that the sharp peak at 395 nm is relatively independent of the crystal lattice.^{9,10} Therefore this peak has been assigned to a transition from ${}^6A_{1g}({}^6S)$ to ${}^4A_{1g}({}^4G)$.^{9,10} The results of MCSCF calculations, as indicated in Table II, reveal a reversal of the ${}^4E_g({}^4G)$ and ${}^4A_{1g}({}^4G)$ term designations relative to these published assignments. Therefore, we assign the sharp peak at 395 nm as due to transitions from the ${}^6A_{1g}({}^6S)$ to ${}^4E_g({}^4G)$ levels. From Table IV we see that the ${}^4E_g({}^4G, {}^4D)$ terms are independent of Dq and after diagonalizing the ${}^4E_g({}^4G, {}^4D)$ matrix, the ${}^4E_g({}^4G)$ - ${}^6A_{1g}({}^6S)$ separation becomes $10B + 5C$. Then assuming a C/B ratio of 4.48,⁹ we calculate $B = 781 \text{ cm}^{-1}$ and $C = 3.498 \times 10^3 \text{ cm}^{-1}$. With these values of B and C , Dq is the only independent parameter. Figure 5 shows the crystal-field splitting diagram for these values of B and C . The energies are presented with respect to the ground state ${}^6A_{1g}({}^6S)$. The dashed line shows the

TABLE V. Experimental and calculated energies using $B = 781 \text{ cm}^{-1}$, $C = 3498 \text{ cm}^{-1}$, and $Dq = 570 \text{ cm}^{-1}$.

Level	Experimental values ^a		Calculated values	
	Energy (cm ⁻¹)	Wavelength (nm)	Energy (cm ⁻¹)	Wavelength (nm)
${}^4T_{1g}({}^4G)$	22675	441	22354	447
${}^4T_{2g}({}^4G)$	24950	400	24570	407
${}^4E_g({}^4G)$	25510	392	25316	395
${}^4A_{1g}({}^4G)$	25316	395	25316	395
${}^4T_{2g}({}^4D)$	29850	335	29766	336
${}^4E_g({}^4D)$	31250	320	30786	325
${}^4T_{1g}({}^4P)$	33898	295	32593	307
${}^4A_{2g}({}^4F)$	41660	240	41693	240
${}^4T_{1g}({}^4F)$	41660	240	42035	238
${}^4T_{2g}({}^4F)$	42735	234	43458	230

^aMcKeever *et al.* (Ref. 9).

value of Dq that gives the best fit to the experimental data of McKeever *et al.*⁹ With the proper crystal-field splitting diagram for $O_h^{(8)}$ symmetry the fitted Dq value is now 570 cm^{-1} instead of the much lower value of 420 cm^{-1} .^{9,10} This brings it more in line with expectations. The numerical values for the experimental energies together with the calculated energies at $Dq = 570\text{ cm}^{-1}$ are given in Table V.

V. SUMMARY

The purpose of this paper was to analyze the Mn absorption spectrum in $\text{CaF}_2:\text{Mn}$ as observed before irradiation by the employment of *ab initio* quantum-chemical techniques to a cluster consisting of an isolated substitutional Mn^{2+} impurity surrounded by eight F^- ions arranged on the corners of a cube. Hence the $[\text{MnF}_8]^{6-}$ cluster was chosen to represent the isolated Mn substitutional impurity in an otherwise perfect crystal.

The methods of UHF, MP2, MP4, and CISD were used to calculate the spin sextet and spin quartet ground states. With the active space consisting of the Mn $3d$ molecular orbitals, the spin quartet excited states were calculated by the MCSCF method. These values were then compared with the ROHF results for the spin sextet ground state to obtain the transition energies. Since the energy levels of $O_h^{(8)}$ Mn in CaF_2 are well known experimentally,^{9,10} this cluster provided a good test case for the MCSCF technique as applied to defects in solids.

After embedding the $[\text{MnF}_8]^{6-}$ cluster in an external point ion field designed to reproduce the Madelung potential difference within the quantum cluster, the UHF results showed that the presence of this external field had little influence on the rather localized Mn d -to- d transitions. Without the external field, the MCSCF calculations for the spin quartet excited states did a better job predicting the relative spacing of the energy levels than it

does predicting the absolute transition energies. The results showed that good agreement with experiment could be obtained only after a rigid shift of the spin quartet levels by -0.647 eV . Some of this shift could be accounted for by the extension into a more highly correlated level of theory such as CISD.

In addition to the above calculations, the crystal-field term splitting diagrams for the eight-coordinated Mn^{2+} impurity in O_h symmetry were calculated. Since previous ligand-field analyses were performed on the basis of $O_h^{(6)}$ symmetry,^{9,10} one aspect of this project was to rework the ligand-field theory for the proper $O_h^{(8)}$ symmetry. The results of this analysis showed a narrowing of the multiplet terms in energy with respect to the $O_h^{(6)}$ result. As a consequence, after fitting the experimental values to the new diagram, the fitted crystal-field parameter Dq increased from 420 cm^{-1} to 570 cm^{-1} .

With the viability of the MCSCF technique for treating the crystal-field spectra of $3d$ ions in ionic crystals established in this work, future research will center around the application of this method to more complicated defect clusters that are not so easily treated by ligand-field theory. One such defect of importance in $\text{CaF}_2:\text{Mn}$ is the radiation induced Mn F -center defect thought to be important in explaining the optical absorption spectra in γ -irradiated $\text{CaF}_2:\text{Mn}$ for use in dosimetry applications.⁹

ACKNOWLEDGMENTS

The authors wish to express their gratitude to Dr. S. W. S. McKeever for many helpful discussions. We would like to thank Konrad Brandermuhl at the Oklahoma State University Computer Center for his generous assistance. This work was funded in part by the Naval Surface Warfare Center under contract No. N60921-89-Q-10-137 and by a grant from the U.S. Dept. of Education No. P-200-A-900-59.

¹ R. J. Ginther and R. D. Kirk, *J. Electrochem. Soc.* **104**, 365 (1957).

² J. H. Schulman, F. H. Attix, E. J. West, and R. J. Ginther, *Rev. Sci. Instrum.* **31**, 1263 (1960).

³ J. H. Schulman, in *Proceedings of the Symposium on Solid State and Chemical Radiation and Dosimetry in Medicine and Biology*, edited by J. H. Schulman (IAEA, Vienna, 1967), p. 3.

⁴ J. H. Schulman, R. J. Ginther, S. G. Gorbics, A. E. Nash, E. J. West, and F. H. Attix, *Int. J. Appl. Radiat. Isotopes* **20**, 523 (1969).

⁵ A. C. Lucas and B. M. Kapsar, *Health Phys.* **27**, 600 (1974).

⁶ R. Alcalá, P. J. Alonso, G. Lalinde, and A. Carretero, *Phys. Status Solidi B* **98**, 315 (1980).

⁷ P. J. Alonso, V. M. Orera, and R. Alcalá, *Phys. Status Solidi B* **99**, 585 (1980).

⁸ D. W. McMasters, B. Jassemnejad, and S. W. S. McKeever, *J. Phys. D* **20**, 1182 (1987).

⁹ S. W. S. McKeever, B. Jassemnejad, J. F. Landreth, and M. D. Brown, *J. Appl. Phys.* **60**, 1124 (1986).

¹⁰ P. J. Alonso and R. Alcalá, *J. Lumin.* **22**, 321 (1981).

¹¹ J. F. Rhodes, R. J. Abbundi, D. Wayne Cooke, V. K. Mathur, and M. D. Brown, *Phys. Rev. B* **31**, 5393 (1985).

¹² S. W. S. McKeever (unpublished).

¹³ P. J. Alonso and R. Alcalá, *J. Lumin.* **21**, 147 (1980).

¹⁴ D. Wayne Cooke, Evangelos P. Gavathas, and M. D. Brown, *J. Appl. Phys.* **54**, 1165 (1983).

¹⁵ B. Jassemnejad, R. J. Abbundi, M. D. Brown, and S. W. S. McKeever, *Phys. Status Solidi A* **108**, 753 (1988).

¹⁶ M. J. Frisch, G. W. Trucks, M. Head-Gordon, P. M. W. Gill, M. W. Wong, J. B. Foresman, B. G. Johnson, H. B. Schlegel, M. A. Robb, E. S. Replogle, R. Gomperts, J. L. Andres, K. Raghavachari, J. S. Binkley, C. Gonzalez, R. L. Martin, D. J. Fox, D. J. Defrees, J. Baker, J. J. P. Stewart, and J. A. Pople, *GAUSSIAN 92* (Gaussian Inc. Pittsburgh, PA, 1992).

¹⁷ S. Sugano, Y. Tanabe, and H. Kamimura, *Multiplets of Transition-Metal Ions in Crystals* (Academic Press, New York, 1970).

¹⁸ C. C. J. Roothaan, *Rev. Mod. Phys.* **23**, 69 (1951); **32**, 179 (1960).

- ¹⁹ W. J. Hehre, L. Radom, R. v. R. Schleyer, and J. A. Pople, *Ab Initio Molecular Orbital Theory* (Wiley, New York, 1986).
- ²⁰ For an advanced review of *ab initio* methods, see *Ab Initio Methods in Quantum Chemistry*, Vol. LXIX of *Advances in Chemical Physics*, edited by K. P. Lawley (Wiley, New York, 1987), Pts. I and II.
- ²¹ A. Szabo and N. S. Ostlund, *Modern Quantum Chemistry* (McGraw-Hill, New York, 1989).
- ²² A. C. Hurley, *Introduction to the Electron Theory of Small Molecules* (Academic Press, New York, 1976).
- ²³ S. Huzinaga, J. Andzelm, M. Klobukowski, E. Radzio-andzelm, Y. Sakai, and H. Tatewaki, *Gaussian Basis Sets for Molecular Calculations* (Elsevier, Amsterdam, 1984).
- ²⁴ E. A. Hylleraas and B. Undheim, *Ann. Phys. (Leipzig)* **65**, 759 (1930); J. K. L. MacDonald, *Phys. Rev.* **43**, 830 (1933).
- ²⁵ A. C. Wahl and G. Das, in *Methods of Electronic Structure Theory*, edited by H. F. Schaefer III (Plenum, New York, 1977), p. 51.
- ²⁶ B. O. Roos, *Adv. Chem. Phys.* **69**, 399 (1987).
- ²⁷ J. H. Barkyoumb and A. N. Mansour, *Phys. Rev. B* **46**, 8768 (1992).
- ²⁸ *Crystals with the Fluorite Structure*, edited by W. Hayes (Oxford University Press, Oxford, 1974).
- ²⁹ S. Wilson, *Adv. Chem. Phys.* **69**, 439 (1987).
- ³⁰ R. F. Wood and T. M. Wilson, in *Defects in Insulating Solids*, edited by V. M. Tuchkevich and K. K. Shvarts (Springer-Verlag, Berlin, 1981), pp. 186–206.
- ³¹ J. W. Richardson and G. J. M. Janssen, *Phys. Rev. B* **39**, 4958 (1989).
- ³² M. Flórez, L. Seijo, and L. Pueyo, *Phys. Rev. B* **34**, 1200 (1986).
- ³³ T. M. Wilson, *Int. J. Quantum Chem. Suppl.* **24**, 187 (1990).
- ³⁴ K. Luth and S. Scheiner, *Int. J. Quantum Chem. Suppl.* **26**, 817 (1992).
- ³⁵ J. E. Del Bene, E. A. Stahlberg, and I. Shavitt, *Int. J. Quantum Chem. Suppl.* **24**, 455 (1990).
- ³⁶ B. Ng and D. J. Newman, *J. Chem. Phys.* **84**, 3291 (1986).
- ³⁷ R. R. Sharma and S. Sundaram, *Solid State Commun.* **33**, 381 (1980).
- ³⁸ R. R. Sharma, M. H. de A. Viccaro, and S. Sundaram, *Phys. Rev. B* **23**, 738 (1981).
- ³⁹ J. Ferguson, E. R. Krausz, and H. J. Guggenheim, *Mol. Phys.* **27**, 577 (1974).
- ⁴⁰ Y. Tanabe and S. Sugano, *J. Phys. Soc. Jpn.* **9**, 753 (1954); **9**, 766 (1954); **11**, 864 (1956).
- ⁴¹ L. E. Orgel, *J. Chem. Phys.* **23**, 1004 (1955); **23**, 1819 (1955); **23**, 1824 (1955).
- ⁴² H. L. Schläfer and G. Gliemann, *Basic Principles of Ligand Field Theory* (Wiley, New York, 1969).
- ⁴³ J. W. Stout, *J. Chem. Phys.* **31**, 709 (1959).
- ⁴⁴ R. K. Bagai and A. V. R. Warriar, *Phys. Status Solidi B* **73**, K123 (1976).
- ⁴⁵ M. T. Barriuso and M. Moreno, *Chem. Phys. Lett.* **112**, 165 (1984).